JMEPEG (2012) 21:1275–1282
DOI: 10.1007/s11665-011-0002-5

1059-9495/$19.00

Investigation of Bulk Damage Progression and Inspection for GFRP Laminate Properties

Joel J. Schubbe and Anthony N. Mucciardi

(Submitted March 14, 2011; in revised form June 28, 2011)

A study has been accomplished to compare bulk material degradation in two graphite fiber-reinforced plastic (GFRP) laminates under cyclical fatigue. This study is the first in a series of experiments to characterize and quantify acoustic response to large-area bulk properties of field systems with hybrid structural composite-metallic systems. Long before failure of load-bearing composite components, stiffness reduction creates loading path changes, potentially overloading or fatiguing metallic substructure. The composite materials used in this study represent potential components and their respective correlation of stiffness changes to acoustic signal degradation through direct area measurement techniques. Specimens tested were fatigued using a sinusoidal waveform at continuous max loading and stress range at 30, 50, 60, and 70% of each layup, and UTS and cyclic stress-strain data were collected over 100,000 cycles to generate discrete levels of stiffness change. Additional specimens were cycled to one million cycles to generate higher levels of damage and determine failure life in specimens examined. All the specimens in this study were 8-ply, woven, 30.5-cm-long, 2.54-cm-wide, 0.297-cm-thick, rectangular specimens. A damage parameter based on material stiffness, as determined by changes in Young's modulus ($D = 1 - E/E_0$), was employed to compare the overall stiffness changes in the specimens. This damage parameter was correlated to ultrasonic scan results to provide a basis for field characterization of bulk material damage and, subsequently, life estimates of in-use structural parts. Examination of these effects showed a strong correlation of back-face signal strength to stiffness degradation in both laminates.

Keywords damage tolerance, durability, fatigue, life prediction, non-destructive evaluation, ultrasonics

1. Introduction

The use of composite materials has been on the rise for many years. Application of these materials in aerospace, automobiles, industry, sports, and even alternative energy systems is intended to provide a structure that is robust enough without the weight of metallic structure. Boeing has introduced its 787 Dreamliner with skins consisting of 100% composite and 50% of the total aircraft weight in these materials (Ref 1). Although strength is a prime consideration for most designs, the hybrid nature of these structures, e.g., composite skins with dissimilar understructure give rise to the question, ''if the compliance (stiffness) of one of the component materials has a marked change during the life of the vehicle, or the part was not properly designed or built to expected loading, what effect will the change have on the life of the vehicle?'' The first step to ''in-field'' assessment of these effects is to quickly assess the state of the composite component as a primary load path member. Second, an analysis must be accomplished to determine life of secondary load-sharing components to determine a safe operating life. Although many methods exist to enable us to detect and assess localized damage in a laminate including delamination, edge damage, or fastener hole integrity, material characteristics, such as stiffness and residual strength elude direct, or in-situ inspection techniques. Extensive characterization measurements unique to part configurations and material are necessary to determine the accuracy of flaw measurements. Understanding of these parameters has challenged engineers for decades.

In the past, point-by-point scanning techniques of the specimen area were labor intensive, time consuming, and impractical (Ref 2-4). There is a need to determine changes and quantify damage to bulk material properties from fatigue-cycled GFRP structure. In-situ monitoring with testing was accomplished by Govada et al. using a combination of acoustic emissions and acoustography. This tedious acousto-ultrasonic NDT method attempted to capture, as a whole, matrix cracking, micro- and macro-delaminations, fiber splits, debonding, fiber breaks, and the overall complex damage state (Ref 5).

Williams and Lampert showed that attenuation of the ultrasonic inspection signal was an effective technique for determining the effects of impact on composite materials (Ref 6). Duke et al. attempted to use the ultrasonic stress wave factor to correlate changes in material properties in the loading direction during applied loads with fringe patterns showing good correlation with degradation of localized areas but they must be employed during loading of the component specimen (Ref 7). This study attempts to correlate the fatigue degradation (damage) of two GFRP lamina, as characterized by bulk stiffness change, using a standard ultrasonic test signal attenuation method to allow for the field-level inspection of

Joel J. Schubbe and **Anthony N. Mucciardi**, Mechanical Engineering Department, US Naval Academy, 590 Holloway Road, Annapolis, MD 21402. Contact e-mail: Schubbe@usna.edu.

skins or components. This inspection has the potential to allow for the life extension or the termination for suspect components if the part has passed a defined threshold of change.

2. Experimental Methodology

2.1 Specimens and Test Set-up

Specimens were cut from 83.8 × 63.5 cm 8-ply (0.112) AS4/977-3 cloth laminate panels to represent a design-conforming ("C" specimens) lamina with reinforcing 0° plies and a non-conforming ("NC" with 0° lamina absent) material. All were fabricated from the same material batch (AS4-6K/977-3, 14mil, 5 harness cloth, MMS 5025, Type 1). Figure 1 shows a specimen configured for testing.

Ultimate tensile strength (UTS) and static stiffness for each layup were determined using standard quasi-static tensile test techniques with untabbed, unnotched, rectangular specimens. Figure 2 shows the examples of static pull test results. Tests were conducted with and without G-10, rectangular, untapered tabs. Though small differences were seen between the tabbed and untabbed specimens, property trends were consistent, and all specimens failed within the test section. Untabbed specimens were ultimately used for this study after tensile testing showed less than a 2% variation tabbed versus untabbed for ultimate lamina strength. In addition, the absence of adhesively bonded tabs reduced potential variability in the fatigue specimen configurations.

The non-conforming material started the study with approximately a 26% strength deficit and a 27% stiffness difference from the conforming material in these initial tests. The failure strengths of the tabbed, conforming and non-conforming specimens were 803 and 602 MPa, respectively, and the failure strengths for the untabbed conforming and non-conforming specimens were 793 and 590 MPa, respectively. Stiffnesses for the untabbed conforming and non-conforming specimens were determined to be 45.8 and 33.5 GPa, respectively, using a linear portion of the dataset with a minimum correlation coefficient of $R^2 = 0.9998$. A MTS 810 electric servo-hydraulic 22 kip test stand with hydraulic wedge grips was employed to load the specimens, and control was accomplished using an external MTS Flex SE Test controller with MTS PC interface software. A variety of damage levels were generated in specimens, and each loading level was repeated in triplicate to examine the level of variation of damage for any given loading level. Each fatigue test was performed at 5 Hz, $R = 0.1$, and damage ($D = 1 - E/E_0$) was generated at loading equivalent to 30-70% of each lamina's UTS as determined by initial tensile tests.

Tapered-edge hydraulic grips were used and clamping loads were adjusted to allow consistent grip and no perceptible slipping under tensile or fatigue loading and with no perceptible damage increase or failure at the grip location. This was determined by initial ultrasonic (UT) scans of the specimens after test. Each specimen (3 at each load and for each lamina configuration) was cycled for 100,000 sinusoidal load cycles (5 Hz) and then scanned for quantification of the ultrasonic signal degradation at the back face. Strain data was taken for both overall (bulk) specimen stiffness and for localized strains (extensometer) at periodic intervals to provide a stiffness history for each specimen during testing. Figure 3 shows a comparison of the early and final stiffness curves for a single specimen. The final damage, D (stiffness change) at 100,000 cycles, was then compared to the UT scans for trends.

Figure 4 displays a full summary of test points for damage level versus cycles (max 100,000). It should be noted that a typical "wear-in" phase is completed between 1,000 and 10,000 cycles. At this point "wear-out" begins, and appreciable damage accumulates. The non-conforming specimens show a significantly higher level of damage relative to load levels than the conforming specimens.

Fig. 1 Test configuration

2.2 Ultrasonic NDE Background

Ultrasonic material analysis and characterization are based on the principle that the motion of any wave will be affected by the medium through which it travels. Thus, changes in one or more of the four measurable parameters associated with the passage of a high-frequency sound wave through a material—transit time, attenuation, scattering, and frequency content—can often be correlated with changes in physical properties, such as hardness, elastic modulus, density, homogeneity, or grain structure (Ref 8-11).

A significant advantage of ultrasonic testing over other material analysis methods is that it can often be performed for materials in-service. High-frequency sound waves can often be successfully transmitted into materials without direct contact through the use of a water bath or water stream as a coupling medium. Measurements can also be performed within closed containers by coupling sound energy through the wall. Because sound waves penetrate through the test specimen, material properties are measured in bulk rather than just on the surface. It is also possible to analyze just one layer of a multi-layer, multi-material fabrication through the use of selective time-gating.

In some applications, ultrasonic data such as velocity can be directly utilized to calculate properties such as elastic modulus. In other cases, ultrasonic testing is a comparative technique,

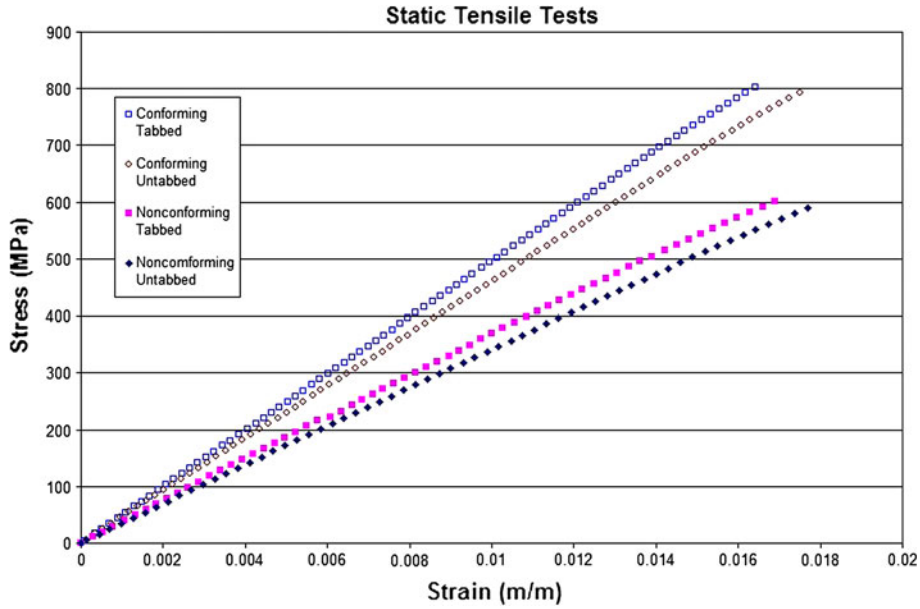

Fig. 2 Tabbed and untabbed specimen tensile test results

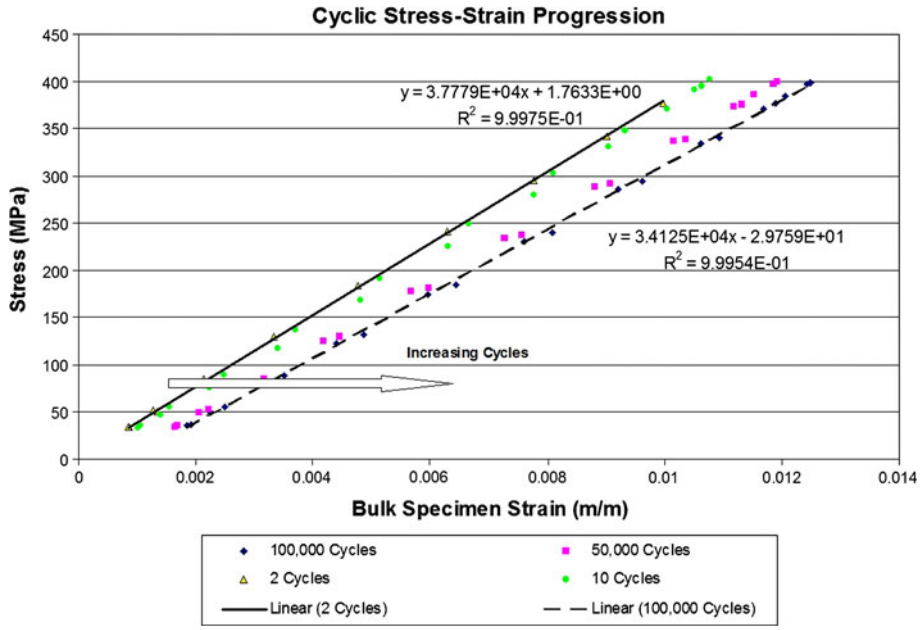

Fig. 3 Stress-strain progression (2-100,000 cycles)

where to establish a test protocol in a given application, it will be necessary to experimentally evaluate reference standards (e.g., undamaged components of the same material under test) representing the range of material conditions being quantified. From such standards, it is possible to detect how sound-transmission parameters vary with changes in specific material properties, and then from this baseline information, how similar changes in test samples can be identified or predicted.

When a sonic wave travels through a medium, its intensity (amplitude) diminishes with distance. In idealized materials, sound pressure (signal amplitude) is only reduced by the spreading of the wave. Natural materials, as well as man-made materials such as composites, however, all produce effects which further weaken the sonic wave's amplitude because of scattering and absorption. Scattering is the reflection of the sonic wave in directions other than its original direction of propagation. Absorption is the conversion of the sonic wave energy to other forms of energy. The combined effect of scattering and absorption is called attenuation. Ultrasonic attenuation is the decay rate of the sonic wave's amplitude, as it propagates through material. Ultrasound propagation through homogeneous media is associated only with absorption and can be characterized with the absorption coefficient only. Propagation through heterogeneous requires taking into account scattering.

Attenuation of sound within a material itself is often not of intrinsic interest. However, natural properties and loading

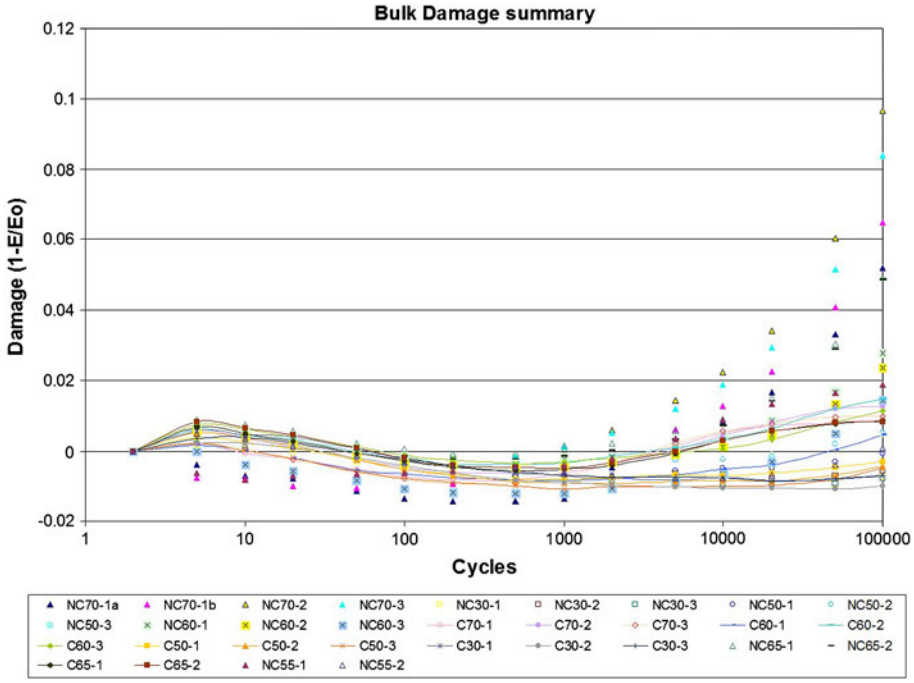

Fig. 4 Summary of specimen damage vs. number of cycles

conditions can be related to attenuation. Attenuation often serves as a measurement tool that leads to the formation of theories to explain physical or chemical phenomenon that decreases the ultrasonic intensity.

In this study, the attenuation (signal amplitude reduction) as the sonic wave propagates through the composite plate with and without damage was measured and used as a key parameter that might relate to damage. Sound energy is absorbed or attenuated in a material governed in a complex fashion by interactive effects of density, hardness, viscosity, and molecular structure. Signal attenuation would likely be correlated with material degradation as the specimens were subjected to increasing tensile test-induced degradation which would quite likely cause a "break up" in the composite matrix, and the resulting matrix structure would show changes in bulk material properties and, hence, in the overall signal attenuation. If true, then this would produce a non-invasive and field-usable UT test that could predict the extent of damage induced by in-service usage to date and provide a means for determining remaining service life.

The amplitude change of a decaying plane wave within a medium can be expressed as (Ref 8):

$$A = A_0 e^{-\alpha z}$$

In this expression, A_0 is the unattenuated amplitude of the propagating wave at some location. The amplitude A is the reduced amplitude after the wave has traveled a distance z from that initial location. The quantity α (expressed in decibels/length) is the attenuation coefficient of the wave traveling in the z-direction.

Attenuation is generally proportional to the square of sound frequency. Quoted values of attenuation are often given for a single frequency, or an attenuation value averaged over many frequencies may also be given. In this study, a broadband, ultrasonic transducer was used whose center frequency is 10 MHz with significant energy in the frequency range of

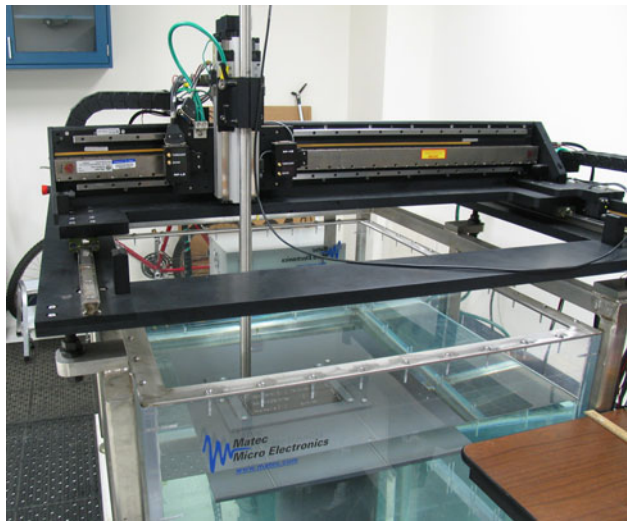

Fig. 5 Ultrasonic scanning tank

±50% of the center frequency. Consequently, in this study, the signal attenuation was a function of the composite material attenuation at each of these frequency components (Ref 8, 9).

2.3 Materials and Methods

Testing was carried out using a Matec ultrasonic immersion tank (MI-Scan IC) which is a high-resolution tank used primarily for acoustic microscopy inspection of electronic components. The ultrasonic sensor/electronics front end consisted of a focused 10-MHz broadband transducer (Panametrics V311) with a focal distance (water) of 6.25 cm interfaced to a square wave pulser/receiver (Panametrics Model 5072PR). The equipment is shown in Fig. 5 and 6.

The vertical (z) axis was adjusted so that the transducer focal point was at the specimen surface. Examples of typical ultrasonic signals are shown in Fig. 7 and 8 for damage conditions. The top figure shows where the three ultrasonic scanning gates were located. The Front Surface Interface following gate was sufficiently wide (in time) to account for any surface deviations from perfectly horizontal as the scan proceeded across the specimen faces. The two Analysis gates were set up such that the left-most gate monitored the body of the specimen (just below the front surface down to just above the bottom surface), and the right-most gate the bottom surface (“back wall”). It turned out that the important information was that resulting from the back wall gate, which measured the total attenuation as the ultrasonic wave traveled through the specimen for each pixel in the 2D scan. It is seen in Figs. 7 and 8 that there is a significant increase in attenuation that is correlated with increasing damage. The immersion tank was programmed to conduct a bi-directional 2D raster scan over an area sufficient to include all five the specimens mounted in the scanning rig. The scan parameters were as follows: Hor Scan Length = 216 mm; Ver Scan Length = 172 mm; Spacing (pixel size) = 100 μm.

The imaging system software contains basic statistical analysis functions with the average ultrasonic amplitude (across the entire specimen) being the most important for our attenuation analysis.

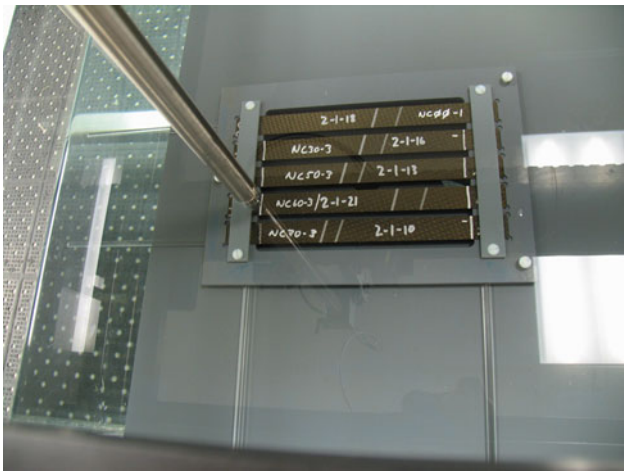

Fig. 6 Specimen scanning rig

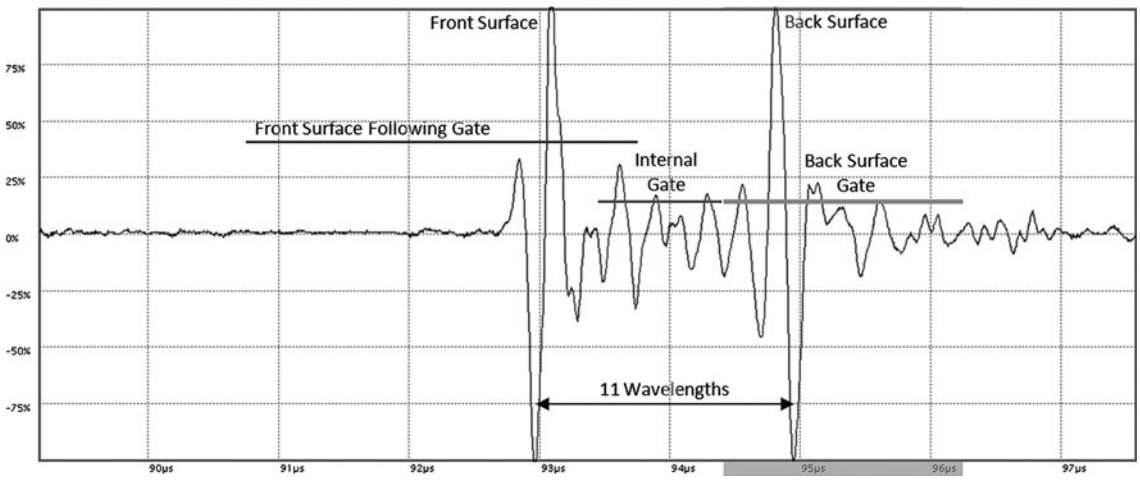

Fig. 7 A-scan image from undamaged specimen

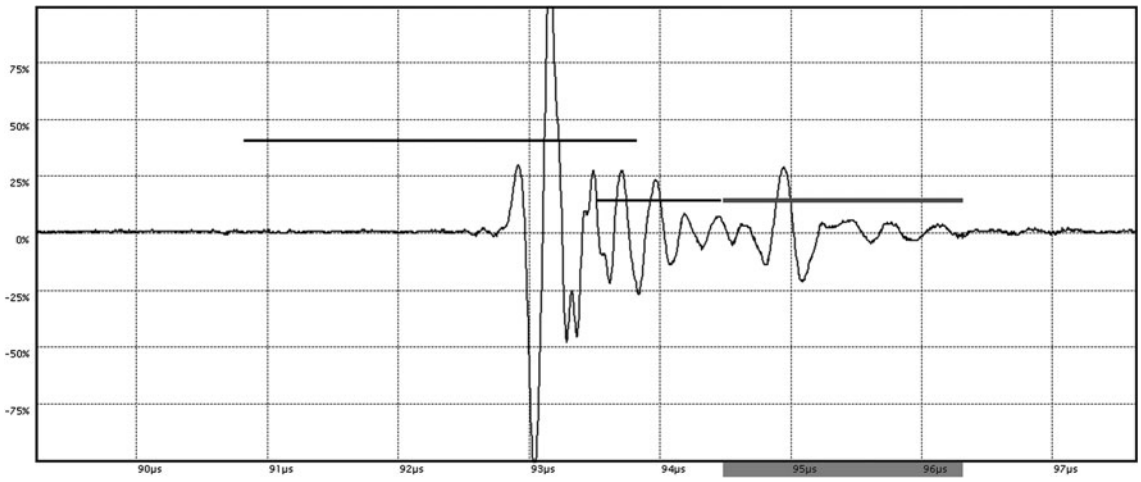

Fig. 8 A-scan image from specimen with 8.4% damage

The results are shown in Fig. 9 where this compilation shows the resulting image for each damage condition along with the test damage quantities. It is seen that no significant change in the image occurs until the damage reaches 1.5% and, from that point onward, there is an increasing and significant change in the image which is strongly correlated with the ultrasonic attenuation non-invasive measurement.

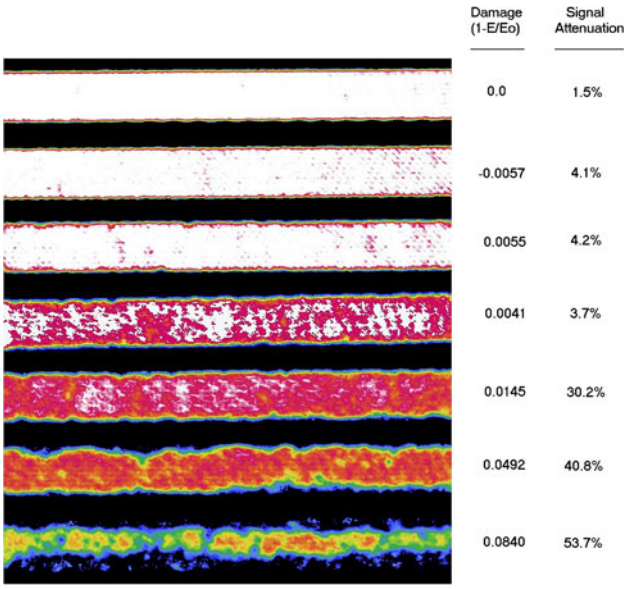

Fig. 9 C-scan image with test results

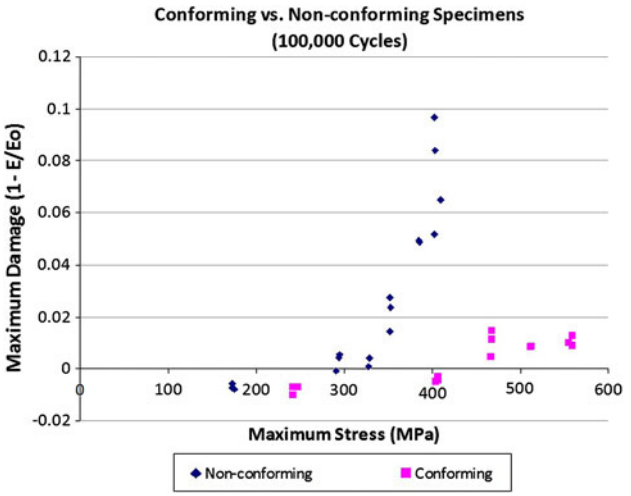

Fig. 10 Measured damage in specimens at 100,000 cycles

Typical reflected UT signals from this GFRP laminate are shown in Fig. 7 and 8. Both undamaged and damaged (8.4% Stiffness Decrease) signals are presented showing the effect of matrix damage on the amplitude of the reflected back wall signal that has traversed throughout the entire body of the specimen. The signal attenuation shown in this figure is typical of the results we obtained during our experiments.

3. Discussion and Results

Maximum damage, as characterized by stiffness change, is shown in Fig. 10. Maximum stiffness change before failure in the conforming specimens' plateaus in the 1-2% range at 100,000 cycles, and it can be concluded that the conforming specimens, having a significant number of 0° plies, are fiber dominated for strain and failure. The non-conforming specimen failure is dominated by progressive damage in the form of matrix micro-cracking or crack progression between plies. It is also seen that there is a clear threshold of stress intensity at approximately 50 GPa that significantly increases the rate of stiffness change, or damage, sustained by each specimen through cyclic fatigue. Figure 11 shows an example of the micro-cracking in the non-conforming specimens. Cracks initiate in the epoxy-rich matrix or in the off-axis plies according as whether the specimens are conforming or non-conforming. No cracking was discernable in the 0º plies or fibers in the specimens examined before failure.

The ultrasonic method employed to evaluate signal degradation for each of the specimens provided digitized C-scan data that were analyzed using an area-averaged method. Approximately 75% of the total image area of each specimen was used to provide an average, a maximum/minimum, and standard deviation values for the signal strength returned at each pixel location. This approach is unique to this study versus previous studies referenced earlier. The aim is not to identify and quantify localized damage, but to provide an assessment of bulk property changes, specifically damage, relative to stiffness change. Figure 12 illustrates the correlation of signal strength with the assessment of stiffness changes in the tests. Signal degradation correlates well for each layup and, despite the curve-fits only being provided for illustrative purposes, they are

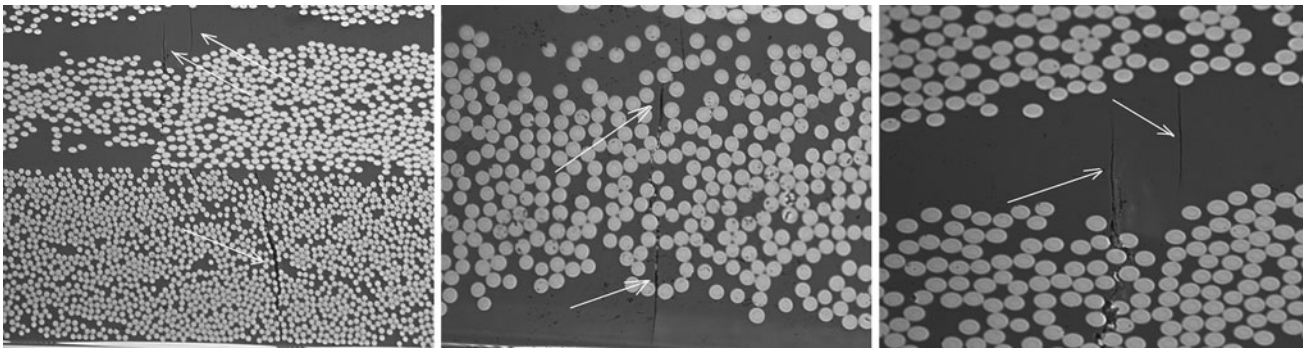

Fig. 11 Micro-cracking in off-axis plies

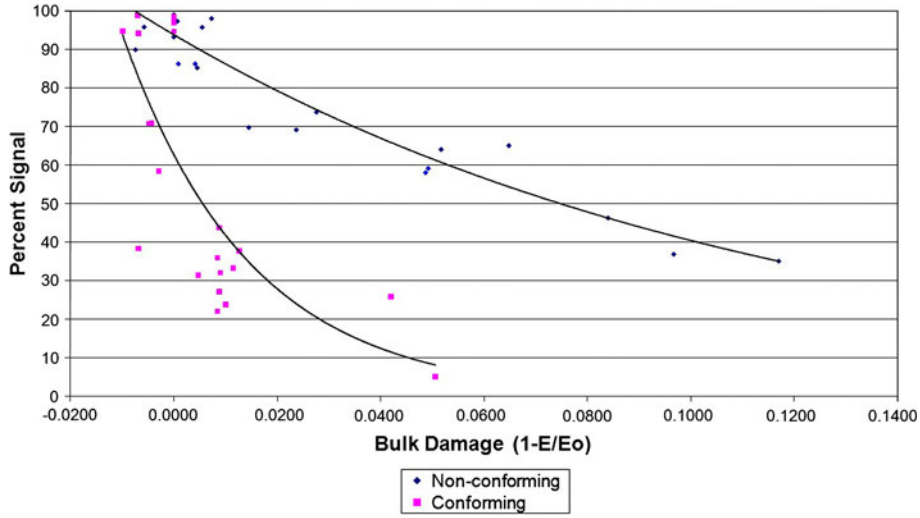

Fig. 12 Signal attenuation with bulk specimen damage

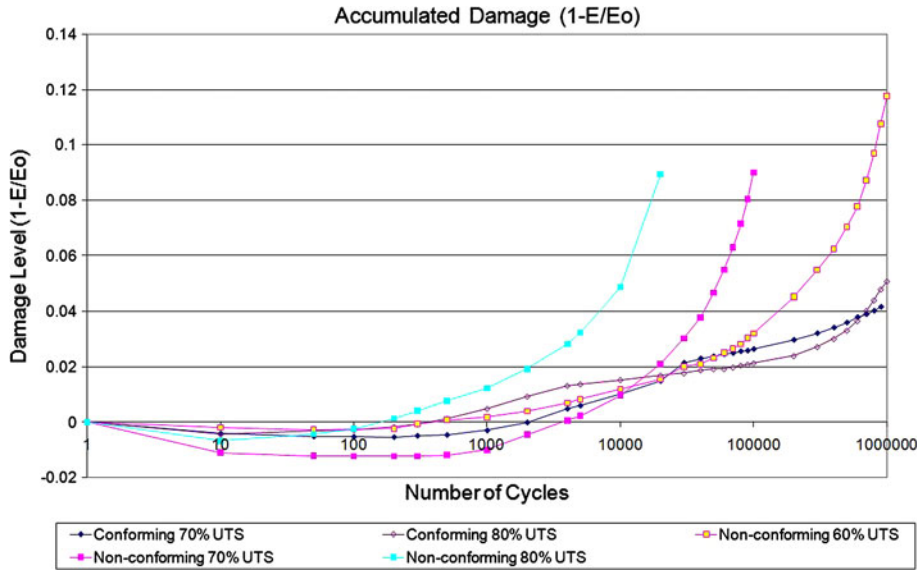

Fig. 13 Specimen-accumulated damage for varied loads (up to 1 million cycles)

easily modeled with the help of a basic exponential function. The non-conforming material has a consistently decreasing signal strength with an increase in damage (decrease in stiffness), but the conforming material plateaus at approximately 1% damage with signal strength continuing to decrease. A sudden jump in damage (near failure) occurs as 0° fibers break. The conclusion that can be drawn is that the matrix and off-axis plies in the conforming material continue to degrade (increasing micro-cracking and voids) with subsequent decreasing signal return. In the absence of 0º fibers in the non-conforming material, stiffness is dominated by progressive damage in the matrix and off-axis fiber plies. The scan signal strength change is much larger than the actual stiffness change and, therefore, provides a sufficient fidelity for measuring the stiffness changes.

For those specimens that were cycled for extended periods of time (1 million cycles or failure), Fig. 13 displays the resulting accumulated damage. Three of these specimens, two conforming and one low-stress non-conforming specimen, did not fail during 1 million cycles of loading. The other non-conforming specimens at higher load levels showed data at failure near 10% damage, with no noticeable plateau present in the data. The third non-conforming specimen, cycled at 60% of UTS, did not fail but exhibited near 12% damage at 1 million cycles. The remaining two conforming specimens plateaued at near 1 or 2% damage until they had undergone more than 100,000 cycles, and did not fail at 1 million cycles.

Data shown in Fig. 14 is provided to give a perspective comparing the two specimen compositions on the basis of applied loading and life. It is clear that the two layups provide different strengths as expected. Except at very high loading conditions, these layups demonstrate similar lives relative to ultimate strength (UTS) and tend to scale well, as shown in Fig. 14. Initial strength and stiffness comparisons show a 26-27% reduction in the non-conforming material. However, as seen in Fig. 12, lack of fibers oriented with loads experienced in operation could potentially add another 12% stiffness change through cyclic fatigue damage. This ultimately means up to a

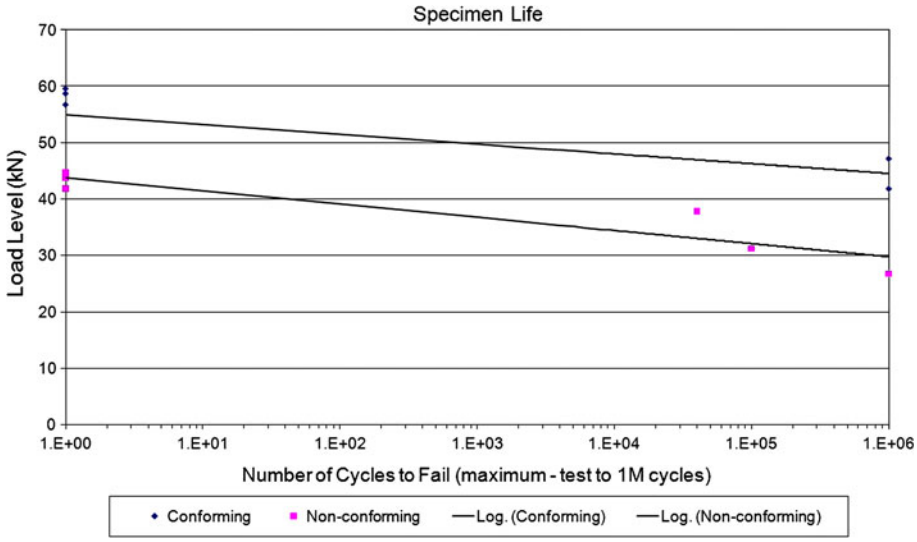

Fig. 14 Load vs. cycles (*S-N*) to 1 million cycles

36% stiffness deficit if operational loads are not aligned with expected predictions.

4. Conclusions

Fatigue life of a graphite-epoxy structural composite is dependent on how well the layup conforms to operational loads and orientation of the same. Misalignment of the fibers or lack of fibers aligned with loading can allow progressive damage to occur in the composite and the experiments in this study show up to a 12% increased degradation of stiffness in the bulk properties of a non-conforming component. Exclusive of localized damage, this phenomenon is a bulk property change, and this study has demonstrated the utility of ultrasonic scanning to provide quantitative correlation with this property change through acoustic signal strength degradation. A follow-up study will include additional calibration for coatings, portable device integration, and signal time-of-flight model integration.

Acknowledgments

This study was supported by the US Navy, Boeing Aerospace, and their respective laboratories. The authors offer special thanks to Dr. Matt Tillman and Mr. Brian Harkless for their support in this research.

References

1. H. Baldwin, 787 Dreamliner™ Unmatched Economics, Performance and Passenger Appeal, *Aviation Week and Space Technology Market Supplement*, Mar 14, 2005
2. J.S. Sandhu, H. Wang, and W.J. Popek, Acoustography for Rapid Ultrasonic Inspection of Composites, *SPIE—International Society for Optical Engineering, Proceedings*, Vol 2944 (Bellingham, WA), 1996, p 117–124
3. A.S. Chen, D.P. Almond, and B. Harris, Acoustography Applied to the Monitoring of Impact Damage Growth in Composites Under Fatigue Conditions, *Acoustical Imaging*, Vol 25, M. Halliwell and P.N.T. Wells, Ed., Kluwer Academic/Plenum Publishers, New York, 2000, p 209–216
4. A.S. Chen, D.P. Almond, and B. Harris, In Situ Monitoring In Real Time of Fatigue-Induced Damage Growth in Composite Materials by Acoustography, *Compos. Sci. Technol.*, 2001, **61**, p 2437–2443
5. A. Govada, E.G. Henneke, and R. Talreda, Acousto-Ultrasonic Measurements to Monitor Damage During Fatigue of Composites, *ASME—Advances in Aerospace Sciences and Engineering*, ASME, New York, NY, 1984, p 55–60
6. J.H. Williams, Jr., and N.R. Lampert, Ultrasonic Evaluation of Impact-Damaged Graphite Fiber Composites, *Mater. Eval.*, 1980, **38**(12), p 68–71
7. J.C. Duke, E.G. Henneke, W.W. Stinchcomb, and K.L. Reifsnider, Characterization of Composite Materials by Means of the Ultrasonic Stress Wave Factor, *Composites 2*, I.H. Marshall, Ed., Applied Science Publishers, London, 1984, p 53–60
8. Anon., *Sound Propagation in Elastic Materials and Attenuation of Sound Waves*, Iowa State University Center for Nondestructive Evaluation NDE Resource Center, Physics of Ultrasound
9. T. Ozturk, O. Kroggel, and P. Grubl, "Propagation of Ultrasound in Concrete—Spatial Distribution and Development of the Young's Modulus, *Proceedings of International Symposium on Non-Destructive Testing in Civil Engineering 2003*, September 16–19, 2003 (Berlin, Germany), 2003
10. M. Posarac, M. Dimitrijevic, J. Majstorovic, T. Volkov-Husovic, and B. Matovic, Nondestructive Testing of Thermal Shock Resistance and Cordierite/Silicon Carbide Composite Materials after Cyclic Thermal Shock, *Res. Nondestr. Eval.*, 2010, **21**, p 1–17
11. S.K. Rathorne, N.N. Kishore, P. Munshi, and W. Arnold, Tomographic Reconstruction of Elastic Constants in Composite Materials Using Numerical and Experimental Laser Ultrasonic Data, *Res. Nondestr. Eval.*, 2010, **21**, p 61–90